

Exploring Applications of Covalent Organic Frameworks: Homogeneous Reticulation of Radicals for Dynamic Nuclear Polarization

Wei Cao,[†] Wei David Wang,[†] Hai-Sen Xu,[†] Ivan V. Sergeyev,[‡] Jochem Struppe,[‡] Xiaoling Wang,[§] Frederic Mentink-Vigier,[§] Zhehong Gan,[§] Ming-Xing Xiao,[†] Lu-Yao Wang,[†] Guo-Peng Chen,[†] San-Yuan Ding,[†] Shi Bai,[⊥] and Wei Wang^{*,†,||}

[†]State Key Laboratory of Applied Organic Chemistry, College of Chemistry and Chemical Engineering, Lanzhou University, Lanzhou, Gansu 730000, China

[‡]Bruker BioSpin Corporation, 15 Fortune Drive, Billerica, Massachusetts 01821, United States

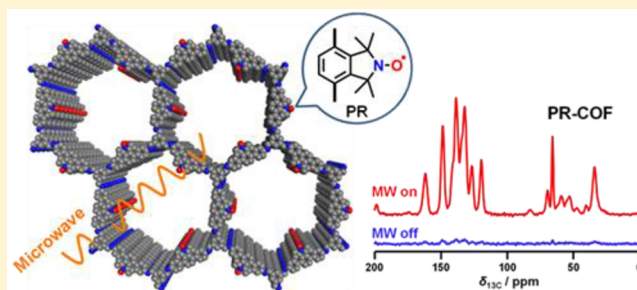
[§]National High Magnetic Field Laboratory, Florida State University, Tallahassee, Florida 32310, United States

[⊥]Department of Chemistry and Biochemistry, University of Delaware, Newark, Delaware 19716, United States

^{||}Collaborative Innovation Center of Chemical Science and Engineering, Tianjin 300071, China

Supporting Information

ABSTRACT: Rapid progress has been witnessed in the past decade in the fields of covalent organic frameworks (COFs) and dynamic nuclear polarization (DNP). In this contribution, we bridge these two fields by constructing radical-embedded COFs as promising DNP agents. Via polarization transfer from unpaired electrons to nuclei, DNP realizes significant enhancement of NMR signal intensities. One of the crucial issues in DNP is to screen for suitable radicals to act as efficient polarizing agents, the basic criteria for which are homogeneous distribution and fixed orientation of unpaired electrons. We therefore envisioned that the crystalline and porous structures of COFs, if evenly embedded with radicals, may work as a new “crystalline sponge” for DNP experiments. As a proof of concept, we constructed a series of proxyl-radical-embedded COFs (denoted as PR(*x*)-COFs) and successfully applied them to achieve substantial DNP enhancement. Benefiting from the bottom-up and multivariate synthetic strategies, proxyl radicals have been covalently reticulated, homogeneously distributed, and rigidly embedded into the crystalline and mesoporous frameworks with adjustable concentration (*x*%). Excellent performance of PR(*x*)-COFs has been observed for DNP ¹H, ¹³C, and ¹⁵N solid-state NMR enhancements. This contribution not only realizes the direct construction of radical COFs from radical monomers, but also explores the new application of COFs as DNP polarizing agents. Given that many radical COFs can therefore be rationally designed and facilely constructed with well-defined composition, distribution, and pore size, we expect that our effort will pave the way for utilizing radical COFs as standard polarizing agents in DNP NMR experiments.

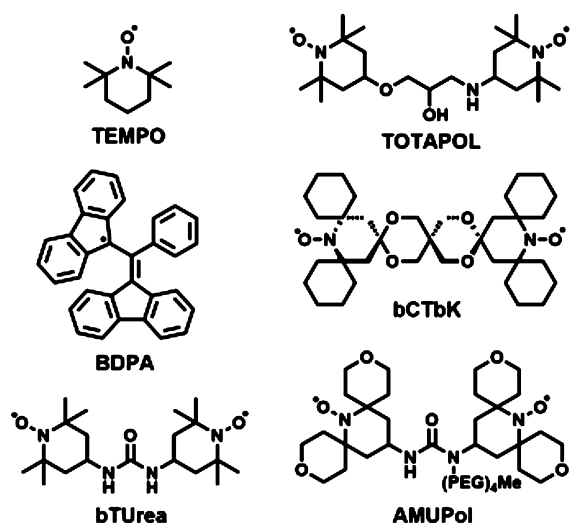


INTRODUCTION

Since the first report in 2005,¹ covalent organic frameworks (COFs)² have attracted increasing interest from various research communities. Precise reticulation of organic building blocks via covalent bonding has rendered COFs with high crystallinity and uniformed porosity. These structural characteristics may further endow COFs with advanced functions. Indeed, potential applications of COFs have been explored in the areas of gas adsorption/separation, catalysis, optoelectricity, sensing, and so on.³ It is therefore expected that crystallinity, porosity, and functionality can be facilely integrated, precisely adjusted, and further utilized for *unique* applications. Toward this goal, we realize herein the application of COFs as efficient agents for dynamic nuclear polarization (DNP).⁴

DNP at high magnetic fields⁵ proved to be a fascinating technique to overcome the intrinsically low sensitivity of NMR spectroscopy: polarization transfer from unpaired electrons to surrounding nuclei can enable enhancement of NMR signal intensities by 2–3 orders of magnitude.^{4m} One of the most critical requirements for DNP is to screen suitable polarizing agents,⁴ⁱ which should possess unpaired electrons and transfer the polarization efficiently. Several organic radicals (Scheme 1) have been found effective⁶ for DNP when physically mixed with the analyte. However, the aggregation of radicals at cryogenic temperatures has hindered^{4g,m} the practical applications of DNP; as a compromise in most cases, glass formers⁷ (such as

Received: March 19, 2018

Scheme 1. Typical Organic (Bi)radicals for DNP NMR Enhancement⁶

glycerol or dimethyl sulfoxide) have to be co-added as indispensable solvents so as to disperse the radicals. A very recent breakthrough to overcome this bottleneck is the exploration of solid polarizing agents.^{8–20} For example, Gajan et al.¹³ recently developed inorganic–organic hybrids in which the TEMPO or bTUrea radicals (Scheme 1) were post-attached to the surface of mesoporous silica. Being free of glass formers, these radical-modified hybrid matrixes proved their efficiency, facility, and recyclability in solid-state DNP NMR experiments. Inspired by these pioneering works, we envisioned taking full advantage of the structural uniqueness of COFs and constructing radical-embedded COFs as new polarizing agents for DNP.

To design an efficient polarizing agent, homogeneous distribution of radicals and fixed *g*-tensor orientation of unpaired electrons are key to the improvement of the so-called cross-effect (CE).^{4f,6e,j} We therefore envisioned that crystalline and porous frameworks such as COFs, if evenly embedded with radicals, would have the following advantages: (i) The *ordered*

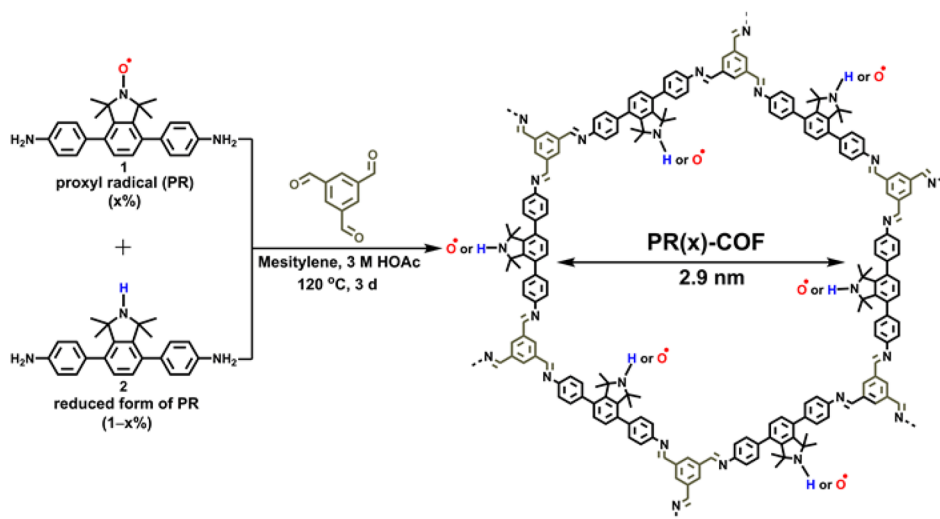
structure ensures homogeneous distribution of radicals throughout the network. (ii) The *rigid* structure helps to fix the orientation of the embedded radicals. (iii) Being free of glass formers, the *porous* structure acts as a “crystalline sponge”²¹ to accommodate the analyte of interest.

Taking all these criteria into account, we achieve herein the direct construction of radical-containing²² COFs from radical monomers. As shown in Scheme 2, a series of proxyl radical (PR) embedded COFs (denoted as PR(*x*)-COFs) have been successfully synthesized, in which the proxyl radicals **1** are homogeneously and rigidly reticulated into the framework via the bottom-up²³ synthetic strategy. In addition, the radical concentration (*x*%, from 0 to 100%) in the framework can be explicitly controlled in the presence of **2** (the reduced form of **1**) by the multivariate²⁴ approach. These criteria²⁵ are crucial for screening the best experimental conditions for DNP enhancement (the concentration issue, *vide infra*). Indeed, benefiting from their structural uniqueness, PR(*x*)-COFs have shown excellent performance as new DNP agents. Specifically, the PR(20)-COF reached an enhancement factor $\epsilon_H \approx 64$ at high magnetic field of 9.4 T. Note that the proxyl radical **1** and its reduced form **2** are new compounds and can be facilely synthesized on a large scale via our method (see Supporting Information (SI) for synthetic details).²⁶ We therefore expect that radical-containing COFs, such as PR(*x*)-COFs, may work as the promising polarizing agents for DNP experiments in the near future.

RESULTS

Designed Synthesis and Structural Characterization.

As briefly mentioned above, the prerequisite for DNP enhancement is that the radicals should be evenly distributed with a suitable inter-radical distance.^{6a,13,27} Too large a distance will decrease the overall rate of polarization transfer, while too short a distance (i.e., radical aggregation) will lead to fast electron relaxation and dramatically lower the polarization efficiency. This dilemma is solved herein by covalent reticulation of radicals into the COF frameworks. Via the multivariate approach shown in Scheme 2, co-condensation of the proxyl radical **1**, its reduced form **2**, and 1,3,5-

Scheme 2. Bottom-Up Construction of PR(*x*)-COFs for DNP NMR Enhancement^a

^aThe radical concentration in the COF framework can be explicitly controlled via the multivariate approach.

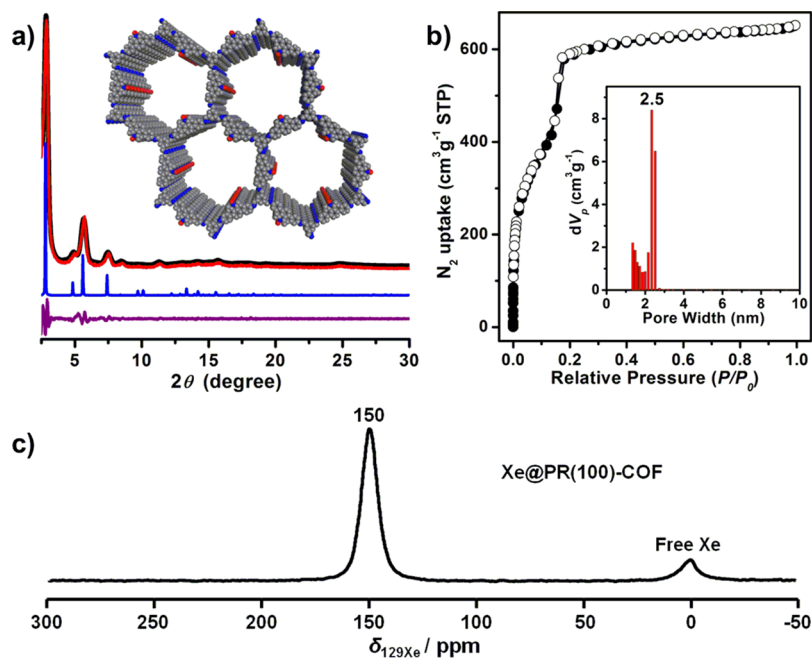


Figure 1. (a) Experimental PXRD pattern (black), Pawley refined pattern (red), difference plot (purple), and simulated pattern (blue) for the eclipsed model of PR(100)-COF. Inset: Extended structure of PR(100)-COF. C, gray; N, blue; O, red; H atoms omitted for clarity. (b) N_2 adsorption (filled symbols) and desorption (empty symbols) isotherms of PR(100)-COF. Inset: pore-size distribution of PR(100)-COF. (c) ^{129}Xe NMR spectrum of PR(100)-COF; the pressure of xenon adsorbed in PR(100)-COF was controlled at 4.1 bar.

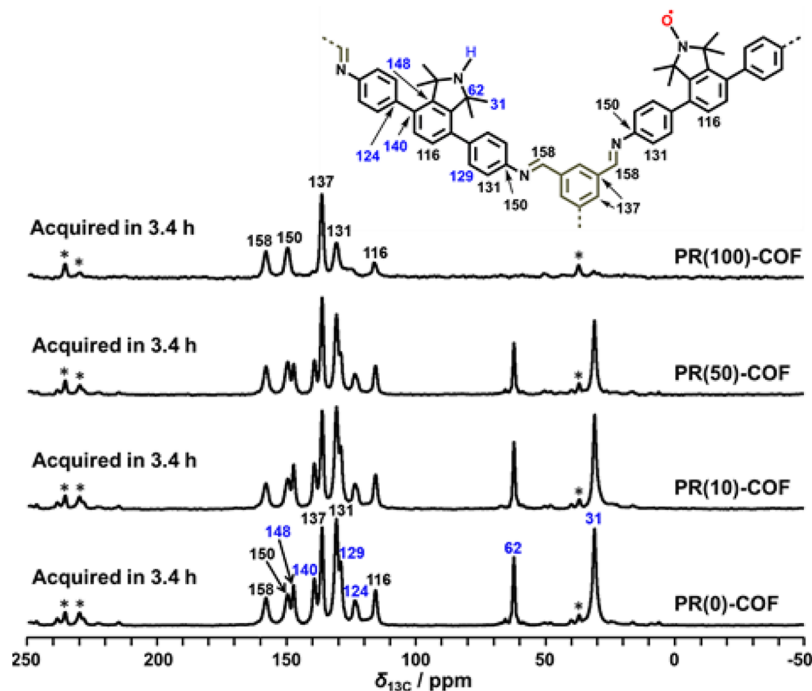


Figure 2. ^{13}C CP/MAS NMR spectra of PR(x)-COFs. Asterisks denote the spinning sidebands. Assignments of ^{13}C chemical shifts of PR(x)-COFs are indicated in the chemical structure. Note that the ^{13}C NMR signals in the radical region (146, 134, 76, 68, and 31 ppm in Figure S41) are absent.

triformylbenzene via imine-bond formation resulted in a series of PR(x)-COFs (see SI for details). The radical concentration in PR(x)-COFs has been finely adjusted by varying the proportion of proxyl radical **1** to its reduced form **2** from the beginning. The characterization results confirmed that PR(x)-COFs are highly crystalline mesoporous materials and the proxyl radicals are homogeneously distributed within the COF frameworks.

The crystalline and porous structure of PR(x)-COFs was verified by powder X-ray diffraction (PXRD) analysis, nitrogen adsorption–desorption isotherm, and ^{129}Xe NMR spectroscopy. PR(x)-COFs with different radical concentrations showed similar PXRD patterns (Figure S6); the structural simulation suggested that they possess preferentially the eclipsed π – π stacking model (Figure 1a). Derived from nitrogen adsorption–desorption data, large Brunauer–Emmett–Teller (BET)

surface areas of 1179–1742 m² g⁻¹ and pore volumes of 0.74–2.0 cm³ g⁻¹ were calculated for PR(*x*)-COFs (Table S2). Moreover, the pore-size distribution of PR(*x*)-COFs is centered at 2.5 nm, which agrees with the theoretical data (2.9 nm) of the pore diameter in the proposed stacking model (Figure 1b). ¹²⁹Xe NMR spectrum for ¹²⁹Xe atoms adsorbed into PR(100)-COF showed only one signal which has the narrow full width at half-maximum of 975 Hz (Figure 1c). These data indicate that the synthesized PR(*x*)-COFs are highly crystalline materials with uniform pores. Importantly, the pore size of PR(*x*)-COFs falls into the mesoporous region, which is large enough to accommodate common analytes.

The covalent connection at atomic level in PR(*x*)-COFs was further elucidated by FT-IR and solid-state NMR spectroscopy. The FT-IR spectra of PR(*x*)-COFs showed the same –C=N– stretch at 1626 cm⁻¹ (Figure S3), indicating the successful formation of imine bonds. In addition, the vibration at 1355 cm⁻¹ represents the typical stretching of nitroxyl radicals. Figure 2 shows the ¹³C cross-polarization magic-angle spinning (CP/MAS) NMR spectra of PR(*x*)-COFs (*x* = 0, 10, 50, 100; more spectra shown in Figure S40). It is worth mentioning that, due to the paramagnetic broadening, radical-containing polymers could hardly be characterized by solid-state NMR spectroscopy.²⁸ Only very few successful examples^{16,28} have been reported in the literature, and the signals were too broad for unambiguous assignments. Herein, the NMR signals are very narrow and, can be assigned explicitly upon the comparison of NMR data for samples with varied radical concentrations. For example, the signal at 158 ppm is characteristic for the carbon atoms of imine bonds. Meanwhile, the signal at 137 ppm should be assigned to the carbon atoms originating from 1,3,5-triformylbenzene, while the signals at 150, 131, and 116 ppm represent the aromatic carbon atoms from monomers 1 and 2. Note that carbon atoms adjacent to NO• radicals are subject to paramagnetic bleaching and therefore, the signals at 148, 140, 129, 124, 62, and 31 ppm should be assigned to the carbon atoms originating from the neutral monomer 2. In addition, the successful embedding of proxyl radicals was verified by magnetic measurements via superconducting quantum interference device (SQUID): the results from the *M*–*H* (Figure S59) and *χ_m*–*T* plots (Figure S60) illustrated the paramagnetic behavior²⁹ of PR(100)-COF.

The homogeneous distribution of radicals in PR(*x*)-COFs has been verified by EPR spectroscopic analysis. Figure 3 presents typical EPR spectra of PR(*x*)-COFs recorded at room temperature (more EPR spectra shown in Figure S42). The EPR spectra of PR(*x*)-COFs with higher radical concentration (*x* = 50 and 100) possess a single line with a Lorentzian line shape due to large spin-exchange interaction,³⁰ while those with lower radical concentration (*x* = 2–35) possess three lines due to strong hyperfine interaction³¹ with ¹⁴N nuclei. The observation of hyperfine splitting in the EPR spectra implies that radicals are largely separated and evenly distributed in PR(*x*)-COFs. Moreover, the radical concentration in each sample was derived from the comparison of the double integral of the EPR signal to that of monomer 1. Note that the radical concentration (*C_{rad}*, from 0.02 to 1.80 mmol g⁻¹) calculated via this method showed linear correlation with the ingredient proportion (*x*%, from 2 to 100%) of the radical monomer 1 (Figure S44). This linear correlation also implies the homogeneous reticulation of radicals into the crystalline framework. The overwhelming evidence for the homogeneous distribution of radicals was obtained from the EPR spectra

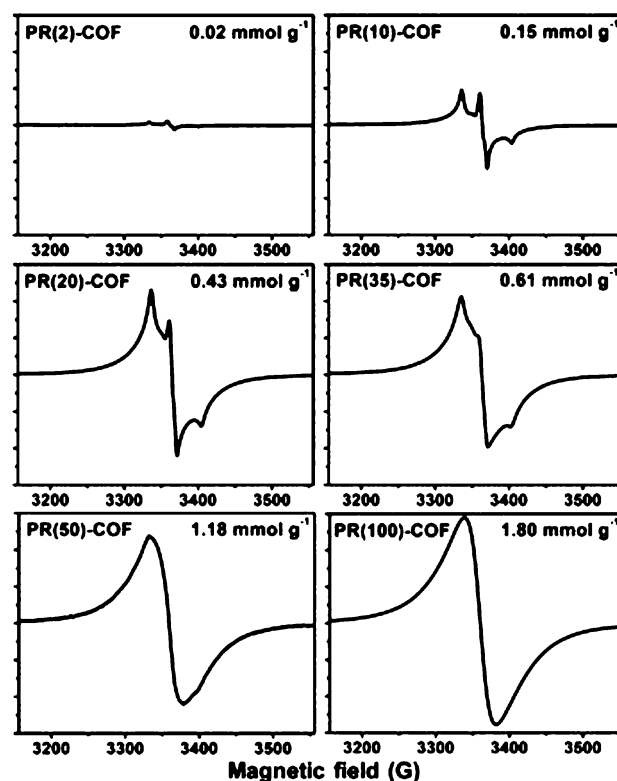


Figure 3. CW X band (9.5 GHz) EPR spectra of PR(*x*)-COFs recorded at 293 K in the solid state. Intensity was corrected for different receiver gain value and power attenuation. Upon the comparison of the double integral of the EPR signal to that of monomer 1, the derived radical concentration (*C_{rad}*, from 0.02 to 1.80 mmol g⁻¹) has been listed on the top right corner in each case. The *C_{rad}* value showed a linear correlation with the ingredient proportion (*x*%, from 2 to 100%) of the radical monomer 1 (Figure S44).

acquired at 110 K for PR(*x*)-COF (*x* = 2–35) samples impregnated with CHCl₃ (Figure S45).³² The central line widths, which were least affected by the *g*-tensor and hyperfine anisotropies, ranged from 10.7 to 13.2 G (Table S3). Note that these line widths are narrower than those of other nitroxide radical materials^{13–16,18} reported, which normally ranged from 12 to 20 G.

PR(*x*)-COFs for DNP Enhancement. With a series of radical embedded PR(*x*)-COFs in hand, we set out to screen the best candidate for DNP enhancement. Accordingly, DNP experiments of PR(*x*)-COFs impregnated with H₂O were performed at 9.4 T and ~100 K and the original spectra have been shown in Figures S65–S76. DNP enhancement was observed for all the measured samples. In the presence of PR(20)-COF, an optimal ¹H DNP enhancement (*ε_H*) of ~64 for the protons from H₂O and ¹³C CP DNP enhancement (*ε_{CP}*) of ~39 for the framework carbons were observed (Figure 4). Meanwhile, we found that DNP enhancement increases upon increasing radical concentration from 0.06 to 0.43 mmol g⁻¹ (*x* = 6–20), which comes from the increased overall rate of electron-to-nucleus polarization transfer. However, with radical concentration increased further from 0.43 to 0.61 mmol g⁻¹ (*x* = 20–35), the DNP enhancement decreases most likely due to faster electron spin cross-relaxation via stronger inter-radical interactions.^{27,33} Similar trends were also observed in other systems by Gajan et al.¹³ and Besson et al.¹⁶

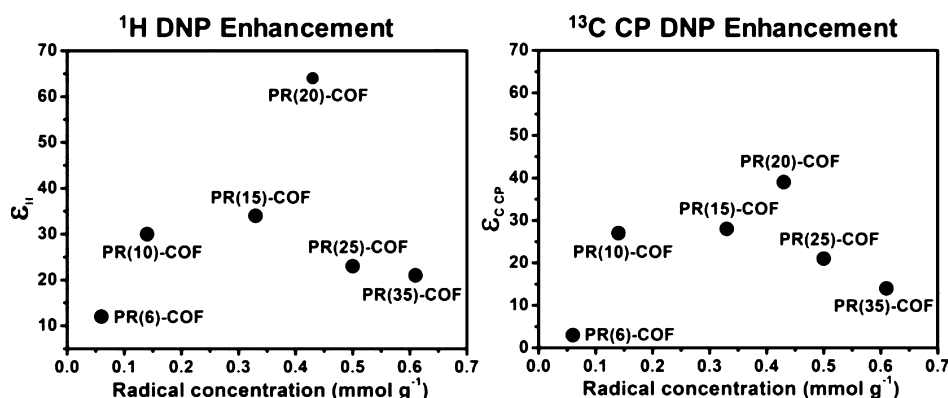


Figure 4. DNP ^1H NMR enhancement (ϵ_{H} , left) and ^{13}C CP NMR enhancement ($\epsilon_{\text{C CP}}$, right) as a function of the radical concentration (C_{rad}) for PR(x)-COFs. DNP ^1H MAS NMR spectra and ^{13}C CP/MAS NMR spectra of PR(x)-COFs impregnated with H_2O were recorded at 9.4 T and ~ 100 K with the microwave field on and off, respectively. The original spectra have been shown in Figures S65–S76.

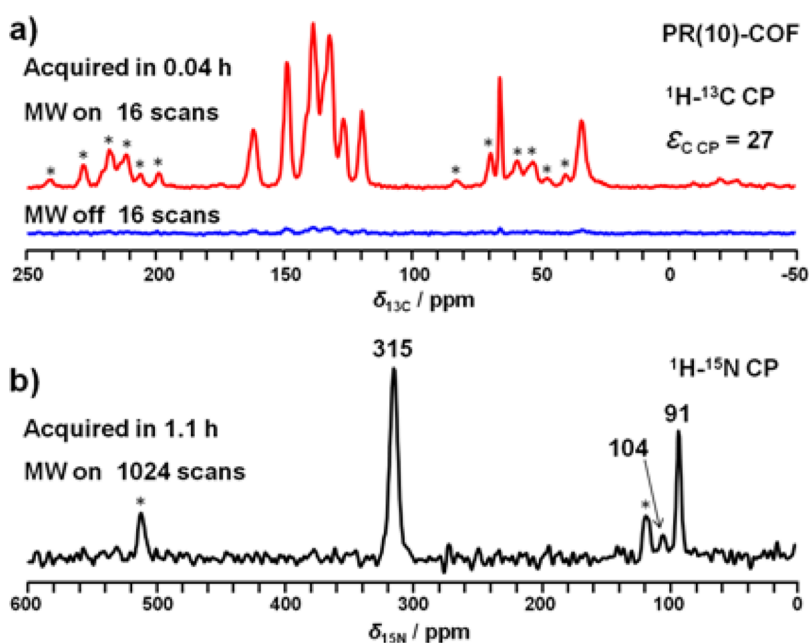


Figure 5. (a) DNP ^{13}C CP/MAS NMR spectrum of PR(10)-COF impregnated with H_2O recorded at 9.4 T and ~ 100 K with the microwave (MW) field on and off, respectively. (b) DNP ^{15}N CP/MAS NMR spectrum of PR(10)-COF impregnated with H_2O recorded at 9.4 T and ~ 100 K with the MW field on. Note that this spectrum could not be acquired without DNP. Asterisks denote the spinning sidebands (spinning rate of 8.0 kHz) in each spectrum.

Figure 5a shows the DNP ^{13}C CP/MAS NMR spectrum of PR(10)-COF impregnated with H_2O with the microwave field on and off, respectively. The spectrum could be recorded with only 16 scans (acquired in 0.04 h) with microwave on. For comparison, with the microwave field off, the corresponding spectrum has to be recorded with 8000 scans (acquired in 3.4 h) to reach reasonable signal-to-noise ratios (see Figure 2). Encouraged by these results, we further collected the ^{15}N CP/MAS NMR spectrum of PR(x)-COF under DNP conditions. This spectrum could not be acquired without DNP. Figure 5b shows the DNP ^{15}N CP/MAS NMR spectrum of PR(10)-COF recorded with 1024 scans only (acquired in 1.1 h). The peaks at 91, 104, and 315 ppm were assigned to the nitrogen atoms of $-\text{N}-\text{H}$, $-\text{N}\text{H}_2$ (terminal), and $-\text{N}=\text{C}-$ bonds, respectively. Again, these results indicate that PR(x)-COF is indeed an efficient DNP polarizing agent.

Finally, the efficiency of PR(x)-COFs for polarizing guest molecules was tested by using $[2,3-^{13}\text{C}]$ -L-alanine as an analyte.

DNP ^{13}C CP/MAS NMR experiment of PR(15)-COF impregnated with 0.1 M H_2O solution of $[2,3-^{13}\text{C}]$ -L-alanine was performed at 9.4 T and ~ 100 K. Figure 6a shows that the ^{13}C resonance of $[2,3-^{13}\text{C}]$ -L-alanine can be effectively enhanced by DNP and a ^{13}C CP DNP enhancement factor of ~ 44 is obtained. The signals at 52 and 18 ppm are due to the labeled carbon atoms originating from $[2,3-^{13}\text{C}]$ -L-alanine.³⁴ This result indicates that, being absorbed in the pores of PR(x)-COFs, the guest molecules, such as $[2,3-^{13}\text{C}]$ -L-alanine can be efficiently polarized by the radicals embedded on the pore walls through proton spin diffusion³⁵ via H_2O . In addition, in order to check whether PR(x)-COFs are efficient polarizing agents at even higher magnetic field, DNP ^{13}C CP/MAS NMR experiment of the same PR(15)-COF was also conducted at 14.1 T and ~ 105 K. Strikingly, a ^{13}C CP DNP enhancement ($\epsilon_{\text{C CP}}$) of ~ 32 was given for the carbons from $[2,3-^{13}\text{C}]$ -L-alanine (Figure 6b). Note that in most of the reported cases,

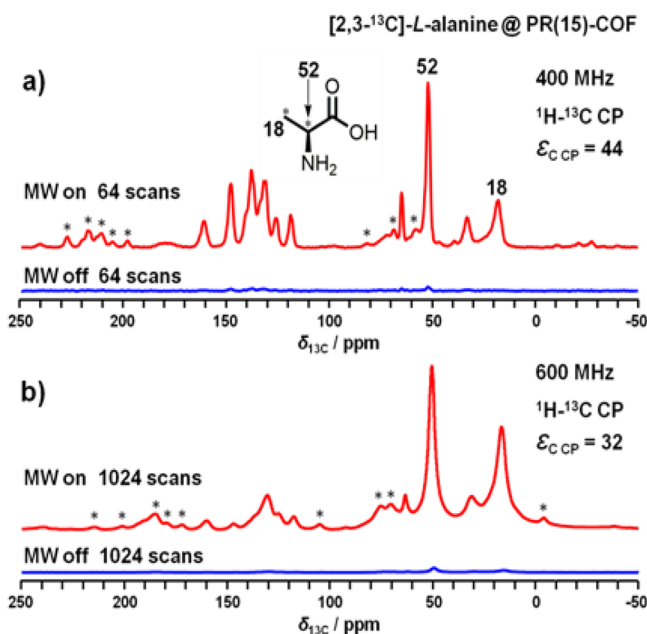


Figure 6. DNP ^{13}C CP/MAS NMR spectra of PR(15)-COF impregnated with 0.1 M H_2O solution of $[2,3-^{13}\text{C}]$ -L-alanine recorded at different magnetic fields of 9.4 T (a) and 14.1 T (b). The spectra were acquired at ~ 100 K/ ~ 105 K with the microwave (MW) field on and off, respectively. Asterisks denote the spinning sidebands (spinning rates of 8.0 and 8.2 kHz, respectively).

however, the DNP efficiency dropped^{6f,i} significantly at higher magnetic fields such as at 14.1 T.

DISCUSSION

The key to exploring advanced applications of new materials is how to utilize their structural uniqueness. This criterion has been exemplified in this contribution by the homogeneous reticulation of radicals into COF structures for DNP enhancement. For this purpose, a series of radical-embedded COFs have been bottom-up synthesized.²² Meeting the demands for an ideal DNP agent, the synthesized COFs, PR(x)-COFs, should have the following structural characteristics: (i) The proxyl radicals are covalently reticulated, homogeneously distributed, and rigidly embedded into the highly ordered crystalline framework. Radical aggregation caused by solvent (such as water) crystallization at cryogenic temperatures is therefore avoided, which is crucial³⁶ for efficient polarization transfer in DNP. (ii) Benefiting from the multivariate approach shown in Scheme 2, a series of PR(x)-COFs can be facilely synthesized with varied radical concentration ($x\%$). This provides an important tool for screening for optimally efficient DNP agents: it has well been acknowledged that the DNP efficiency is indeed sensitive^{13,33,37} to the concentration of radicals. (iii) PR(x)-COFs possess well-defined mesopores with the diameter of ca. 2.5 nm which not only act as ideal hosts²¹ for analytes but also facilitate¹⁵ the transfer of polarization via spin diffusion.

All these structural features have rendered PR(x)-COFs new and promising polarizing matrixes in DNP applications. (i) The EPR data not only verified the homogeneous distribution of proxyl radicals in PR(x)-COFs, but also gave narrow line widths ranging from 10.7 to 13.2 G. These properties have proven important for an efficient DNP agent. (ii) DNP ^1H enhancement was observed at 9.4 T and ~ 100 K for PR(x)-

COFs impregnated with H_2O . An optimal ^1H DNP enhancement (ϵ_{H}) of ~ 64 for the protons from H_2O was obtained with PR(20)-COF. We therefore conclude that polarization can be efficiently transferred within the straight channels from the unpaired electrons of PR(x)-COFs to the hydrogen nuclei of water. (iii) Both ^{13}C and ^{15}N CP DNP enhancements of PR(x)-COFs were observed at 9.4 T and ~ 100 K. An optimal ^{13}C CP DNP enhancement ($\epsilon_{\text{C CP}}$) of ~ 39 was observed for the framework carbons of PR(20)-COF. Notably, as shown in Figure 5b, the ^{15}N CP/MAS NMR spectra could not be acquired without DNP. These results indicate that the polarization can be further transferred from ^1H nuclei to the carbon or nitrogen nuclei within PR(x)-COFs frameworks. (iv) The ability of PR(x)-COFs to polarize different guest molecules was demonstrated. With $[2,3-^{13}\text{C}]$ -L-alanine as the analyte, the ^{13}C CP DNP enhancement ($\epsilon_{\text{C CP}}$) of ~ 44 was observed at 9.4 T and of ~ 32 was observed at 14.1 T.

The advantages of using radical-containing COFs for DNP enhancement are evident. Given that many strategies have been established in recent years for the covalent construction of COFs, a diverse range of radical-containing COFs can be rationally designed and facilely synthesized with well-defined composition, distribution, and pore size. With the availability of these crystalline porous structures, further investigation on the structure–performance relationship is possible, the information from which will certainly shed new light in DNP research. In addition, being structurally robust and totally insoluble in solvents, radical-containing COFs can be easily recycled for repeated use by removal of the analytes. Therefore, these radical-containing COFs should also be intrinsically suitable for dissolution DNP^{14,20,38} measurements; a solution of analytes can be readily separated from the polarizing agent immediately after polarization.

CONCLUSION

With its ability to dramatically improve the sensitivity of NMR spectroscopy, dynamic nuclear polarization has evolved in recent years into a broadly useful and fascinating technique. By taking advantage of the structural uniqueness of COFs, we explore herein a new application for these agile materials: as efficient DNP agents. For this purpose, a series of proxyl-radical-embedded COFs, PR(x)-COFs, have been bottom-up constructed with highly ordered crystalline structures and large BET surface areas. The covalent reticulation, homogeneous distribution, and rigid fixation of proxyl radicals with controlled concentrations are all advantageous for DNP enhancement. Indeed, DNP ^1H , ^{13}C CP, and ^{15}N CP DNP enhancements of PR(x)-COFs were successfully observed at 9.4 T and even at a higher magnetic field of 14.1 T. Given that radical-containing COFs can be facilely and diversely synthesized as two- or three-dimensional crystalline structures, as well as easily scaled-up, we expect that our contribution will boost the unique application of crystalline COFs as glass-former-free agents for DNP experiments.

ASSOCIATED CONTENT

Supporting Information

The Supporting Information is available free of charge on the ACS Publications website at DOI: 10.1021/jacs.8b02839.

Detailed synthetic procedures, FT-IR spectra, PXRD patterns, modeling details and atomic coordinates, N_2 adsorption–desorption isotherms, solid-state NMR

spectra, EPR spectra, TGA traces, SEM images, SQUID measurements, and DNP NMR experiments, including Figures S1–S79 and Tables S1–S5 (PDF)
X-ray crystallographic data for proxyl radical **1** (CIF)

AUTHOR INFORMATION

Corresponding Author

*wang_wei@lzu.edu.cn

ORCID

Frederic Mentink-Vigier: 0000-0002-3570-9787

San-Yuan Ding: 0000-0003-2160-4092

Wei Wang: 0000-0002-9263-7927

Notes

The authors declare no competing financial interest.

ACKNOWLEDGMENTS

This work was mainly supported by the National Natural Science Foundation of China (Nos. 21425206 and 21632004). A portion of this work was performed at the National High Magnetic Field Laboratory, which is supported by National Science Foundation Cooperative Agreement No. DMR-1157490* and the State of Florida. The 14.1 T DNP system at NHMFL is funded in part by NIH P41 GM122698 and S10 OD018519 (magnet and console), and NSF CHE-1229170 (gyrotron). The international collaboration has also been supported by the 111 project (No. 111-2-17) and the International Joint Research Centre for Green Catalysis and Synthesis, Gansu Provincial Sci. & Tech. Department (No. 2016B01017).

REFERENCES

- (1) Côté, A. P.; Benin, A. I.; Ockwig, N. W.; O’Keeffe, M.; Matzger, A. J.; Yaghi, O. M. *Science* **2005**, *310*, 1166.
- (2) For reviews, see: (a) Feng, X.; Ding, X.; Jiang, D. *Chem. Soc. Rev.* **2012**, *41*, 6010. (b) Ding, S.-Y.; Wang, W. *Chem. Soc. Rev.* **2013**, *42*, 548. (c) Colson, J. W.; Dichtel, W. R. *Nat. Chem.* **2013**, *5*, 453. (d) Waller, P. J.; Gándara, F.; Yaghi, O. M. *Acc. Chem. Res.* **2015**, *48*, 3053. (e) Slater, A. G.; Cooper, A. I. *Science* **2015**, *348*, aaa8075. (f) Huang, N.; Wang, P.; Jiang, D. *Nat. Rev. Mater.* **2016**, *1*, 16068. (g) Segura, J. L.; Mancheno, M. J.; Zamora, F. *Chem. Soc. Rev.* **2016**, *45*, 5635. (h) Jiang, J.; Zhao, Y.; Yaghi, O. M. *J. Am. Chem. Soc.* **2016**, *138*, 3255. (i) Diercks, C. S.; Yaghi, O. M. *Science* **2017**, *355*, eaal1585. (j) Rogge, S. M. J.; Bavykina, A.; Hajek, J.; Garcia, H.; Olivios-Suarez, A. I.; Sepulveda-Escribano, A.; Vimont, A.; Clet, G.; Bazin, P.; Kapteijn, F.; Daturi, M.; Ramos-Fernandez, E. V.; Llabres i Xamena, F. X.; Van Speybroeck, V.; Gascon, J. *Chem. Soc. Rev.* **2017**, *46*, 3134. (k) Jin, Y.; Hu, Y.; Zhang, W. *Nat. Rev. Chem.* **2017**, *1*, 0056. (l) Beuerle, F.; Gole, B. *Angew. Chem., Int. Ed.* **2018**, *57*, 4850.
- (3) A more comprehensive list of references is presented in the SI. For selected examples, see: (a) Han, S. S.; Furukawa, H.; Yaghi, O. M.; Goddard, W. A. *J. Am. Chem. Soc.* **2008**, *130*, 11580. (b) Ding, S.-Y.; Gao, J.; Wang, Q.; Zhang, Y.; Song, W.-G.; Su, C.-Y.; Wang, W. *J. Am. Chem. Soc.* **2011**, *133*, 19816. (c) Ding, X.; Guo, J.; Feng, X.; Honsho, Y.; Guo, J.; Seki, S.; Maitarak, P.; Saeki, A.; Nagase, S.; Jiang, D. *Angew. Chem., Int. Ed.* **2011**, *50*, 1289. (d) Yu, J.-T.; Chen, Z.; Sun, J.; Huang, Z.-T.; Zheng, Q.-Y. *J. Mater. Chem.* **2012**, *22*, 5369. (e) DeBlase, C. R.; Silberstein, K. E.; Truong, T.-T.; Abruña, H. D.; Dichtel, W. R. *J. Am. Chem. Soc.* **2013**, *135*, 16821. (f) Bertrand, G. H. V.; Michaelis, V. K.; Ong, T.-C.; Griffin, R. G.; Dinca, M. *Proc. Natl. Acad. Sci. U. S. A.* **2013**, *110*, 4923. (g) Dogru, M.; Handloser, M.; Auras, F.; Kunz, T.; Medina, D.; Hartschuh, A.; Knochel, P.; Bein, T. *Angew. Chem.* **2013**, *125*, 2992. (h) Chandra, S.; Kundu, T.; Kandambeth, S.; BabaRao, R.; Marathe, Y.; Kunjir, S. M.; Banerjee, R. *J. Am. Chem. Soc.* **2014**, *136*, 6570. (i) Fang, Q.; Wang, J.; Gu, S.; Kaspar, R. B.; Zhuang, Z.; Zheng, J.; Guo, H.; Qiu, S.; Yan, Y. *J. Am. Chem. Soc.* **2015**, *137*, 8352. (j) Wang, X.; Han, X.; Zhang, J.; Wu, X.; Liu, Y.; Cui, Y. *J. Am. Chem. Soc.* **2016**, *138*, 12332. (k) Sun, Q.; Aguila, B.; Perman, J.; Nguyen, N.; Ma, S. *J. Am. Chem. Soc.* **2016**, *138*, 15790. (l) Ma, H.; Liu, B.; Li, B.; Zhang, L.; Li, Y.-G.; Tan, H.-Q.; Zang, H.-Y.; Zhu, G. *J. Am. Chem. Soc.* **2016**, *138*, 5897. (m) Yin, Z.-J.; Xu, S.-Q.; Zhan, T.-G.; Qi, Q.-Y.; Wu, Z.-Q.; Zhao, X. *Chem. Commun.* **2017**, *53*, 7266. (n) Lu, S.; Hu, Y.; Wan, S.; McCaffrey, R.; Jin, Y.; Gu, H.; Zhang, W. *J. Am. Chem. Soc.* **2017**, *139*, 17082. (o) Banerjee, T.; Haase, F.; Savasci, G.; Gottschling, K.; Ochsenfeld, C.; Lotsch, B. V. *J. Am. Chem. Soc.* **2017**, *139*, 16228. (p) Li, Z.; Li, H.; Guan, X.; Tang, J.; Yusran, Y.; Li, Z.; Xue, M.; Fang, Q.; Yan, Y.; Valtchev, V.; Qiu, S. *J. Am. Chem. Soc.* **2017**, *139*, 17771. (4) For the earliest reports, see: (a) Overhauser, A. W. *Phys. Rev.* **1953**, *92*, 411. (b) Carver, T. R.; Slichter, C. P. *Phys. Rev.* **1953**, *92*, 212. For selected reviews, see: (c) Morley, G. W.; van Tol, J.; Ardavan, A.; Porfyraakis, K.; Zhang, J.; Briggs, G. A. *Phys. Rev. Lett.* **2007**, *98*, 220501. (d) Maly, T.; Debelouchina, G. T.; Bajaj, V. S.; Hu, K. N.; Joo, C. G.; Mak-Jurkauskas, M. L.; Sirigiri, J. R.; van der Wel, P. C.; Herzfeld, J.; Temkin, R. J.; Griffin, R. G. *J. Chem. Phys.* **2008**, *128*, 052211. (e) Griesinger, C.; Bennati, M.; Vieth, H. M.; Luchinat, C.; Parigi, G.; Hofer, P.; Engelke, F.; Glaser, S. J.; Denysenkov, V.; Prisner, T. F. *Prog. Nucl. Magn. Reson. Spectrosc.* **2012**, *64*, 4. (f) Hovav, Y.; Feintuch, A.; Vega, S. *J. Magn. Reson.* **2012**, *214*, 29. (g) Rossini, A. J.; Zagdoun, A.; Lelli, M.; Lesage, A.; Copéret, C.; Emsley, L. *Acc. Chem. Res.* **2013**, *46*, 1942. (h) Franck, J. M.; Pavlova, A.; Scott, J. A.; Han, S. *Prog. Nucl. Magn. Reson. Spectrosc.* **2013**, *74*, 33. (i) Keshari, K. R.; Wilson, D. M. *Chem. Soc. Rev.* **2014**, *43*, 1627. (j) Kobayashi, T.; Perras, F. A.; Slowing, I. I.; Sadow, A. D.; Pruski, M. *ACS Catal.* **2015**, *5*, 7055. (k) Lee, D.; Hediger, S.; De Paëpe, G. *Solid State Nucl. Magn. Reson.* **2015**, *66–67*, 6. (l) Smith, A. N.; Long, J. R. *Anal. Chem.* **2016**, *88*, 122. (m) Lilly Thankamony, A. S.; Wittmann, J. J.; Kaushik, M.; Corzilius, B. *Prog. Nucl. Magn. Reson. Spectrosc.* **2017**, *102–103*, 120. (5) A more comprehensive list of references is presented in the SI. For selected examples, see: (a) Prandolini, M. J.; Denysenkov, V. P.; Gafurov, M.; Endeward, B.; Prisner, T. F. *J. Am. Chem. Soc.* **2009**, *131*, 6090. (b) Salnikov, E.; Rosay, M.; Pawsey, S.; Ouari, O.; Tordo, P.; Bechinger, B. *J. Am. Chem. Soc.* **2010**, *132*, 5940. (c) Corzilius, B.; Smith, A. A.; Barnes, A. B.; Luchinat, C.; Bertini, I.; Griffin, R. G. *J. Am. Chem. Soc.* **2011**, *133*, 5648. (d) Lee, D.; Takahashi, H.; Thankamony, A. S.; Dacquain, J. P.; Bardet, M.; Lafon, O.; Paepé, G. *J. Am. Chem. Soc.* **2012**, *134*, 18491. (e) Blanc, F.; Sperrin, L.; Jefferson, D. A.; Pawsey, S.; Rosay, M.; Grey, C. P. *J. Am. Chem. Soc.* **2013**, *135*, 2975. (f) Wolf, P.; Valla, M.; Rossini, A. J.; Comas-Vives, A.; Nunez-Zarur, F.; Malaman, B.; Lesage, A.; Emsley, L.; Coperet, C.; Hermans, I. *Angew. Chem., Int. Ed.* **2014**, *53*, 10179. (g) Valla, M.; Rossini, A. J.; Caillot, M.; Chizallet, C.; Raybaud, P.; Digne, M.; Chaumonnot, A.; Lesage, A.; Emsley, L.; van Bokhoven, J. A.; Coperet, C. *J. Am. Chem. Soc.* **2015**, *137*, 10710. (h) Lilly Thankamony, A. S.; Lion, C.; Pourpoint, F.; Singh, B.; Perez Linde, A. J.; Carnevale, D.; Bodenhausen, G.; Vezin, H.; Lafon, O.; Polshettivar, V. *Angew. Chem., Int. Ed.* **2015**, *54*, 2190. (i) Perras, F. A.; Kobayashi, T.; Pruski, M. *J. Am. Chem. Soc.* **2015**, *137*, 8336. (j) Mollica, G.; Dekhil, M.; Ziarelli, F.; Thureau, P.; Viel, S. *Angew. Chem., Int. Ed.* **2015**, *54*, 6028. (k) Mouat, A. R.; George, C.; Kobayashi, T.; Pruski, M.; van Duyne, R. P.; Marks, T. J.; Stair, P. C. *Angew. Chem., Int. Ed.* **2015**, *54*, 13346. (l) Potapov, A.; Yau, W. M.; Ghirlando, R.; Thurber, K. R.; Tycko, R. *J. Am. Chem. Soc.* **2015**, *137*, 8294. (m) Kaplan, M.; Narasimhan, S.; de Heus, C.; Mance, D.; van Doorn, S.; Houben, K.; Popov-Celeketic, D.; Damman, R.; Katrukha, E. A.; Jain, P.; Geerts, W. J. C.; Heck, A. J. R.; Folkers, G. E.; Kapitein, L. C.; Lemeer, S.; van Bergen En Henegouwen, P. M. P.; Baldus, M. *Cell* **2016**, *167*, 1241. (n) Stoppler, D.; Song, C.; van Rossum, B. J.; Geiger, M. A.; Lang, C.; Mroginiski, M. A.; Jagtap, A. P.; Sigurdsson, S. T.; Matysik, J.; Hughes, J.; Oschkinat, H. *Angew. Chem., Int. Ed.* **2016**, *55*, 16017. (o) Kaminker, I.; Shimon, D.; Hovav, Y.; Feintuch, A.; Vega, S. *Phys. Chem. Chem. Phys.* **2016**, *18*, 11017. (p) Ji, X.; Bornet, A.; Vuichoud, B.; Milani, J.; Gajan, D.; Rossini, A. J.; Emsley, L.; Bodenhausen, G.; Jannin, S. *Nat. Commun.* **2017**, *8*, 13975. (q) Berruyer, P.; Lelli, M.; Conley, M. P.; Silverio, D. L.; Widdifield, C. M.; Siddiqi, G.; Gajan, D.; Lesage, A.; Coperet, C.; Emsley, L. *J. Am. Chem. Soc.* **2017**, *139*, 849. (r) Saliba, E. P.; Sesti, E.

L.; Scott, F. J.; Albert, B. J.; Choi, E. J.; Alaniva, N.; Gao, C.; Barnes, A. *B. J. Am. Chem. Soc.* **2017**, *139*, 6310.

(6) (a) Koelsch, C. F. *J. Am. Chem. Soc.* **1957**, *79*, 4439. (b) Hu, K.-N.; Yu, H.-h.; Swager, T. M.; Griffin, R. G. *J. Am. Chem. Soc.* **2004**, *126*, 10844. (c) Song, C.; Hu, K.-N.; Joo, C.-G.; Swager, T. M.; Griffin, R. G. *J. Am. Chem. Soc.* **2006**, *128*, 11385. (d) Hu, K.-N.; Song, C.; Yu, H.-h.; Swager, T. M.; Griffin, R. G. *J. Chem. Phys.* **2008**, *128*, 052302. (e) Matsuki, Y.; Maly, T.; Ouari, O.; Karoui, H.; Le Moigne, F.; Rizzato, E.; Lyubenova, S.; Herzfeld, J.; Prisner, T.; Tordo, P.; Griffin, R. G. *Angew. Chem.* **2009**, *121*, S096. (f) Sauvée, C.; Rosay, M.; Casano, G.; Aussenac, F.; Weber, R. T.; Ouari, O.; Tordo, P. *Angew. Chem.* **2013**, *125*, 11058. (g) Zagdoun, A.; Casano, G.; Ouari, O.; Schwarzwälder, M.; Rossini, A. J.; Aussenac, F.; Yulikov, M.; Jeschke, G.; Copéret, C.; Lesage, A.; Tordo, P.; Emsley, L. *J. Am. Chem. Soc.* **2013**, *135*, 12790. (h) Liu, Y.; Villamena, F. A.; Rockenbauer, A.; Song, Y.; Zweier, J. L. *J. Am. Chem. Soc.* **2013**, *135*, 2350. (i) Mathies, G.; Caporini, M. A.; Michaelis, V. K.; Liu, Y.; Hu, K.-N.; Mance, D.; Zweier, J. L.; Rosay, M.; Baldus, M.; Griffin, R. G. *Angew. Chem., Int. Ed.* **2015**, *54*, 11770. (j) Kubicki, D. J.; Casano, G.; Schwarzwälder, M.; Abel, S.; Sauvée, C.; Ganesan, K.; Yulikov, M.; Rossini, A. J.; Jeschke, G.; Copéret, C.; Lesage, A.; Tordo, P.; Ouari, O.; Emsley, L. *Chem. Sci.* **2016**, *7*, 550.

(7) Ong, T. C.; Mak-Jurkauskas, M. L.; Walsh, J. J.; Michaelis, V. K.; Corzilius, B.; Smith, A. A.; Clausen, A. M.; Cheetham, J. C.; Swager, T. M.; Griffin, R. G. *J. Phys. Chem. B* **2013**, *117*, 3040.

(8) Gitti, R.; Wild, C.; Tsiao, C.; Zimmer, K.; Glass, T. E.; Dorn, H. C. *J. Am. Chem. Soc.* **1988**, *110*, 2294.

(9) McCarney, E. R.; Han, S. *J. Magn. Reson.* **2008**, *190*, 307.

(10) Dollmann, B. C.; Junk, M. J. N.; Drechsler, M.; Spiess, H. W.; Hinderberger, D.; Munnemann, K. *Phys. Chem. Chem. Phys.* **2010**, *12*, 5879.

(11) Vitzthum, V.; Borcard, F.; Jannin, S.; Morin, M.; Miéville, P.; Caporini, M. A.; Sienkiewicz, A.; Gerber-Lemaire, S.; Bodenhausen, G. *ChemPhysChem* **2011**, *12*, 2929.

(12) Lilly Thankamony, A. S.; Lafon, O.; Lu, X.; Aussenac, F.; Rosay, M.; Trébosc, J.; Vezin, H.; Amoureux, J.-P. *Appl. Magn. Reson.* **2012**, *43*, 237.

(13) Gajan, D.; Schwarzwälder, M.; Conley, M. P.; Grüning, W. R.; Rossini, A. J.; Zagdoun, A.; Lelli, M.; Yulikov, M.; Jeschke, G.; Sauvée, C.; Ouari, O.; Tordo, P.; Veyre, L.; Lesage, A.; Thieuleux, C.; Emsley, L.; Copéret, C. *J. Am. Chem. Soc.* **2013**, *135*, 15459.

(14) Gajan, D.; Bornet, A.; Vuichoud, B.; Milani, J.; Melzi, R.; van Kalker, H. A.; Veyre, L.; Thieuleux, C.; Conley, M. P.; Grüning, W. R.; Schwarzwälder, M.; Lesage, A.; Copéret, C.; Bodenhausen, G.; Emsley, L.; Jannin, S. *Proc. Natl. Acad. Sci. U. S. A.* **2014**, *111*, 14693.

(15) Baudouin, D.; van Kalker, H. A.; Bornet, A.; Vuichoud, B.; Veyre, L.; Cavailles, M.; Schwarzwälder, M.; Liao, W. C.; Gajan, D.; Bodenhausen, G.; Emsley, L.; Lesage, A.; Jannin, S.; Copéret, C.; Thieuleux, C. *Chem. Sci.* **2016**, *7*, 6846.

(16) Besson, E.; Ziarelli, F.; Bloch, E.; Gerbaud, G.; Queyroy, S.; Viel, S.; Gastaldi, S. *Chem. Commun.* **2016**, *52*, 5531.

(17) Cheng, T.; Mishkovsky, M.; Junk, M. J. N.; Münnemann, K.; Comment, A. *Macromol. Rapid Commun.* **2016**, *37*, 1074.

(18) Grüning, W. R.; Bieringer, H.; Schwarzwälder, M.; Gajan, D.; Bornet, A.; Vuichoud, B.; Milani, J.; Baudouin, D.; Veyre, L.; Lesage, A.; Jannin, S.; Bodenhausen, G.; Thieuleux, C.; Copéret, C. *Helv. Chim. Acta* **2017**, *100*, e1600122.

(19) Silverio, D. L.; van Kalker, H. A.; Ong, T.-C.; Baudin, M.; Yulikov, M.; Veyre, L.; Berruyer, P.; Chaudhari, S.; Gajan, D.; Baudouin, D.; Cavailles, M.; Vuichoud, B.; Bornet, A.; Jeschke, G.; Bodenhausen, G.; Lesage, A.; Emsley, L.; Jannin, S.; Thieuleux, C.; Copéret, C. *Helv. Chim. Acta* **2017**, *100*, e1700101.

(20) Cavailles, M.; Bornet, A.; Jaurand, X.; Vuichoud, B.; Baudouin, D.; Baudin, M.; Veyre, L.; Bodenhausen, G.; Dumez, J. N.; Jannin, S.; Coperet, C.; Thieuleux, C. *Angew. Chem., Int. Ed.* **2018**, DOI: 10.1002/anie.201801009.

(21) The “crystalline sponge” is initially referred to crystalline and porous hosts which can accommodate organic molecules (analytes), so that the host–guest system becomes observable by conventional X-ray

structural analysis. This method plays an important role in the absolute structure determination of natural products and their derivatives. See, for example: (a) Inokuma, Y.; Arai, T.; Fujita, M. *Nat. Chem.* **2010**, *2*, 780. (b) Inokuma, Y.; Yoshioka, S.; Ariyoshi, J.; Arai, T.; Hitora, Y.; Takada, K.; Matsunaga, S.; Rissanen, K.; Fujita, M. *Nature* **2013**, *495*, 461. (c) Vinogradova, E. V.; Muller, P.; Buchwald, S. L. *Angew. Chem., Int. Ed.* **2014**, *53*, 3125. (d) Lee, S.; Kapustin, E. A.; Yaghi, O. M. *Science* **2016**, *353*, 808. (e) Öhrström, L. *Science* **2016**, *353*, 754. (f) Hoshino, M.; Khutia, A.; Xing, H.; Inokuma, Y.; Fujita, M. *IUCr* **2016**, *3*, 139. (g) Matsuda, Y.; Mitsunashi, T.; Lee, S.; Hoshino, M.; Mori, T.; Okada, M.; Zhang, H.; Hayashi, F.; Fujita, M.; Abe, I. *Angew. Chem., Int. Ed.* **2016**, *55*, 5785. (h) Easun, T. L.; Moreau, F.; Yan, Y.; Yang, S.; Schroder, M. *Chem. Soc. Rev.* **2017**, *46*, 239.

(22) Only three reported examples are relevant to the radical-containing COFs, in all of which, however, post-modification of the neutral COFs with TEMPO radicals or free electrons was applied as the synthetic strategy. See: (a) Xu, F.; Xu, H.; Chen, X.; Wu, D.; Wu, Y.; Liu, H.; Gu, C.; Fu, R.; Jiang, D. *Angew. Chem., Int. Ed.* **2015**, *54*, 6814. (b) Hughes, B. K.; Braunecker, W. A.; Bobela, D. C.; Nanayakkara, S. U.; Reid, O. G.; Johnson, J. C. *J. Phys. Chem. Lett.* **2016**, *7*, 3660. (c) Jin, E.; Asada, M.; Xu, Q.; Dalapati, S.; Addicoat, M. A.; Brady, M. A.; Xu, H.; Nakamura, T.; Heine, T.; Chen, Q.; Jiang, D. *Science* **2017**, *357*, 673.

(23) Du, X.; Sun, Y.; Tan, B.; Teng, Q.; Yao, X.; Su, C.; Wang, W. *Chem. Commun.* **2010**, *46*, 970.

(24) (a) Chen, X.; Addicoat, M.; Jin, E.; Zhai, L.; Xu, H.; Huang, N.; Guo, Z.; Liu, L.; Irlé, S.; Jiang, D. *J. Am. Chem. Soc.* **2015**, *137*, 3241. (b) Pang, Z.-F.; Xu, S.-Q.; Zhou, T.-Y.; Liang, R.-R.; Zhan, T.-G.; Zhao, X. *J. Am. Chem. Soc.* **2016**, *138*, 4710. (c) Crowe, J. W.; Baldwin, L. A.; McGrier, P. L. *J. Am. Chem. Soc.* **2016**, *138*, 10120. (d) Huang, N.; Zhai, L.; Couprie, D. E.; Addicoat, M. A.; Okushita, K.; Nishimura, K.; Heine, T.; Jiang, D. *Nat. Commun.* **2016**, *7*, 12325. (e) Zhang, J.; Han, X.; Wu, X.; Liu, Y.; Cui, Y. *J. Am. Chem. Soc.* **2017**, *139*, 8277.

(25) As previously reported (see ref 24 for examples), the bottom-up and multivariate approaches guaranteed the homogeneous distribution of monomers in the COF frameworks. Meanwhile, the narrow central line widths in the EPR spectra (Table S3) are indicative of the homogeneous distribution of radicals, the issue of which has been specifically demonstrated in the literature (see refs 13 15, and 18). In addition, Figure S58 presents the elemental mapping images which show the homogeneous distribution of O element (mainly originated from NO[•] radicals) as well.

(26) Chinese Patent Appl. No. 201810074645.8, 2018.

(27) Mentink-Vigier, F.; Akbey, U.; Oschkinat, H.; Vega, S.; Feintuch, A. *J. Magn. Reson.* **2015**, *258*, 102.

(28) Behrends, F.; Wagner, H.; Studer, A.; Niehaus, O.; Pöttgen, R.; Eckert, H. *Macromolecules* **2013**, *46*, 2553.

(29) Zhang, J.; Shen, H.; Song, W.; Wang, G. *Macromolecules* **2017**, *50*, 2683.

(30) Wertz, J. E.; Bolton, J. R. *Electron Spin Resonance*; Chapman and Hall: New York, 1986.

(31) Schlick, S. *Advanced ESR Methods in Polymer Research*; Wiley-Interscience: Hoboken, NJ, 2006.

(32) The reason for measuring EPR spectra at 110 K is that the DNP NMR experiments were conducted at cryogenic temperatures. We also conducted EPR measurements on PR(15)-COF impregnated with different solvents at 110 K. The results indicated that solvents with similar polarity had negligible influence on the central line width (Table S4).

(33) (a) Lange, S.; Linden, A. H.; Akbey, Ü.; Trent Franks, W.; Loening, N. M.; Rossum, B.-J. v.; Oschkinat, H. *J. Magn. Reson.* **2012**, *216*, 209. (b) Rossini, A. J.; Zagdoun, A.; Lelli, M.; Gajan, D.; Rascon, F.; Rosay, M.; Maas, W. E.; Coperet, C.; Lesage, A.; Emsley, L. *Chem. Sci.* **2012**, *3*, 108. (c) Takahashi, H.; Fernandez-de-Alba, C.; Lee, D.; Maurel, V.; Gambarelli, S.; Bardet, M.; Hediger, S.; Barra, A. L.; De Paepe, G. *J. Magn. Reson.* **2014**, *239*, 91.

(34) Note that these values are identical to the intrinsic chemical shifts of alanine, indicating that the presence of PR(15)-COF as the host does not distort the structural information of the analytes.

Meanwhile, making the difference spectrum (Figure S79 as an example) can deduct the NMR signals of PR(x)-COFs in the cases that the analytes coincidentally possess similar ^{13}C chemical shifts. In addition, deuteration of PR(x)-COFs should further reduce the background signals and increase the polarizing efficiency.

(35) (a) van der Wel, P. C. A.; Hu, K.-N.; Lewandowski, J.; Griffin, R. G. *J. Am. Chem. Soc.* **2006**, *128*, 10840. (b) Lafon, O.; Thankamony, A. S. L.; Kobayashi, T.; Carnevale, D.; Vitzthum, V.; Slowing, I. I.; Kandel, K.; Vezin, H.; Amoureux, J.-P.; Bodenhausen, G.; Pruski, M. J. *Phys. Chem. C* **2013**, *117*, 1375.

(36) Le, D.; Casano, G.; Phan, T. N. T.; Ziarelli, F.; Ouari, O.; Aussenac, F.; Thureau, P.; Mollica, G.; Gigmes, D.; Tordo, P.; Viel, S. *Macromolecules* **2014**, *47*, 3909.

(37) Lesage, A.; Lelli, M.; Gajan, D.; Caporini, M. A.; Vitzthum, V.; Míéville, P.; Alauzun, J.; Roussey, A.; Thieuleux, C.; Mehdi, A.; Bodenhausen, G.; Coperet, C.; Emsley, L. *J. Am. Chem. Soc.* **2010**, *132*, 15459.

(38) Bornet, A.; Jannin, S. *J. Magn. Reson.* **2016**, *264*, 13.